Ročník 2008 ElectroScope ISSN 1802 – 4564 Číslo 2

Electric Drive with Linear Permanent Magnet Synchronous Motor Current State of Research

J. Vittek[1], V. Vavrúš[1], J. Michalík[1], J. Kuchta[2], M. Rapšík[1]
[1] Department of Power Electrical Systems, Faculty of Electrical Engineering, University of Žilina, Univerzitná 1, 010 26 Žilina, SK
[2] Electrotechnical Research and Development Institute, Trenčianska 19, 018 51 Nová Dubnica, SK
e-mail: jan.vittek@fel.uniza.sk, jan.michalik@fel.uniza.sk, jozef.kuchta@evpu.sk

Abstract:
Current state of research in the area of linear synchronous motor control is presented. Two control methods, vector control and forced dynamics control, are described for speed control of the drive. Both methods offer a dynamic speed response profile, which can be selected for given application by the user. In addition to this, the angle between stator current and moving part magnetic flux vectors is maintained mutually perpendicular to maximize force of the machine. To achieve prescribed speed response during forced dynamics control derived control law requires the external force information, which is obtained from observer. The observer outputs are position, speed, acceleration and external force, which can be exploited for both control techniques and also for diagnostic purpose. Simulations and preliminary experimental results confirm the intended performance of the drive.

INTRODUCTION

The paper develops two control systems for speed and position control of linear permanent magnet synchronous motor (*LPMSM*), which enable to prescribe acceleration of the drive and such a way substantially contribute to the gentle load handling or to the travel comfort during speed-up and braking conditions. As the first stage of research speed control of the drive under vector control (*SVC*) and forced dynamics control (*FDC*) conditions is described.

SVC of the drive with LPMSM is based on the decomposition of the motor into two separately controlled parts [1]. One of them contains channel for machine flux control and the second one contains channel for the force control. In spite of that conventional vector control method can prescribe the shape of acceleration the settling time of the overall control system will always depends on external forces during speed transients. The overall control system for vector control of LPMSM has a nested structure shown in Fig. 1. This structure consist of speed control loop with PI regulator which determines current of force component and control loop for magnetic flux control with PI regulator which controls magnetic flux of the machine.

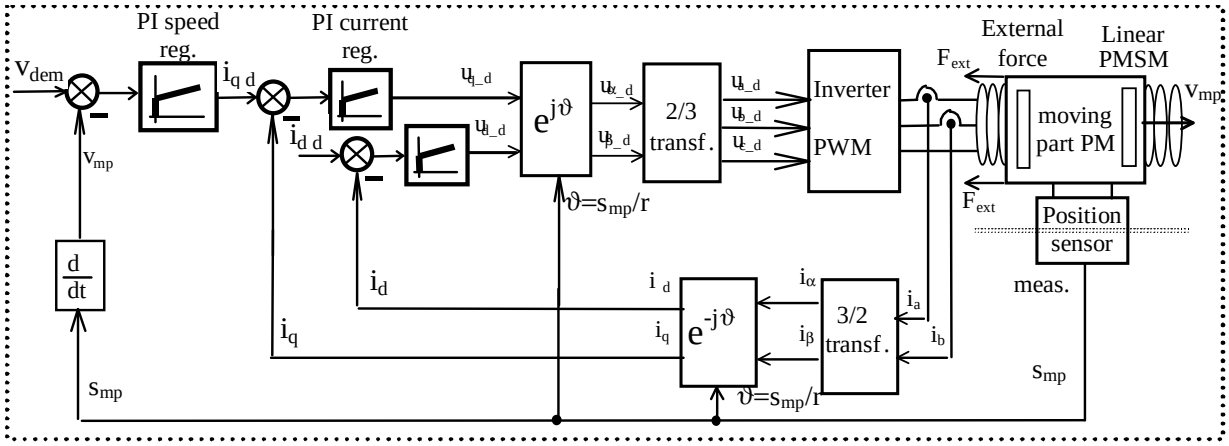

Fig. 1. Overall Vector Control LPMSM control system block diagram

Second control method based on FDC is a form of feedback linearisation [2]. The main reason to utilize this method is that it enables to design such control algorithms, where the settling time of the control system including the shape of acceleration is precisely defined while respecting vector control conditions [3]. To achieve prescribed settling time during speed transients the information about external force acting on moving part is needed. Estimate of the external force together with the moving part position and speed estimates are obtained from the observer, which is full-state observer, correction loops of which are based on the measured position. The overall control system for LPMSM has a nested structure shown in Fig. 2, comprising an outer master control loop and inner slave control loop. Outer master loop computes such demanded stator currents, which realise the closed loop prescribed dynamic

behaviour of the drive. The slave control loop forces the real three-phase stator currents to follow their computed demands from master algorithm with negligible lag via control of power electronic switches.

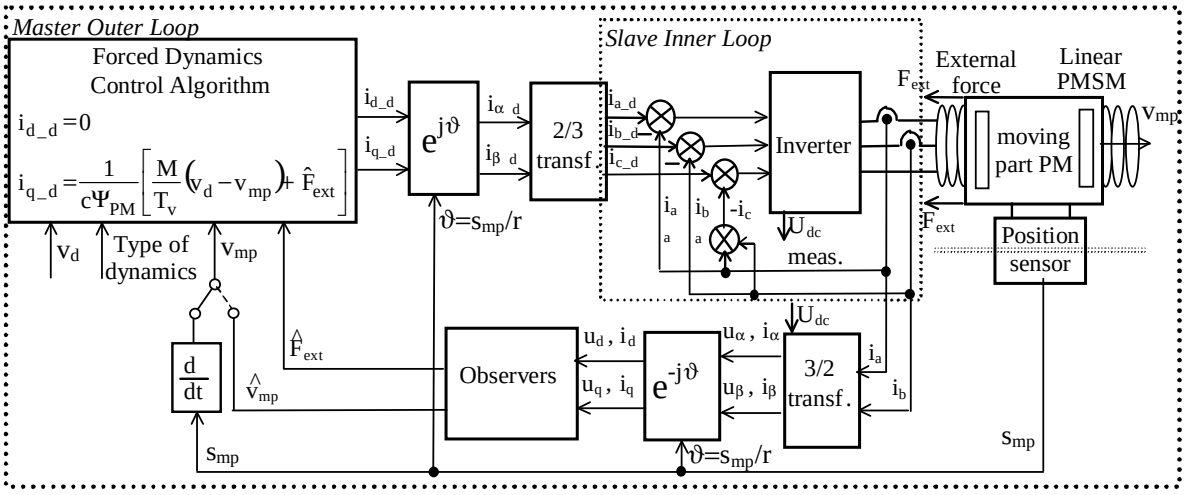

Fig. 2. Overall Forced Dynamics Control of LPMSM block diagram

Both control algorithms utilize model of LPMSM, which is formulated in *d_q* co-ordinate system coupled with moving part of the LPMSM:

$$\frac{ds_{mp}}{dt}=v_{mp} \tag{1}$$

$$\frac{dv_{mp}}{dt}=\frac{1}{M}\left[c\left(\Psi_d i_q-\Psi_q i_d\right)-F_{ext}\right] \tag{2}$$

$$\frac{d}{dt}\begin{bmatrix}i_d\\ i_q\end{bmatrix}=\begin{bmatrix}-R_s/L_d & pv_{mp}L_q/rL_d\\ -pv_{mp}L_d/rL_q & -R_s/L_q\end{bmatrix}\begin{bmatrix}i_d\\ i_q\end{bmatrix} - \frac{pv_{mp}}{rL_q}\begin{bmatrix}0\\ \Psi_{PM}\end{bmatrix}+\begin{bmatrix}1/L_d & 0\\ 0 & 1/L_q\end{bmatrix}\begin{bmatrix}u_d\\ u_q\end{bmatrix} \tag{3}$$

where, $[\,i_d,\ i_q\,]^T$ and $[\,u_d,\ u_q\,]^T$ are, respectively, column vectors of the LPMSM stator current and stator voltage components, s_{mp} and v_{mp} are the position and velocity of the moving part, $c=3p/2r$ where p is number of motor pole-pairs and r is a constant parameter of LPMSM, which depends on the linear motor structure having the dimensions of length, F_{ext} is the external force, R_s is the phase resistance, L_d and L_q are the direct and quadrature phase inductances, Ψ_{PM} is the permanent magnet linkage flux and M is the mass of the linear motor moving part plus the equivalent mass of the driven mechanism.

CONTROL ALGORITHMS DESIGN

Development of LPMSM SVC Algorithm

The basic principle of vector control strategy for the LPMSM is decomposition of a primary part phase current vector into two orthogonal components. The first component, i_d current *produces a magnetizing flux*. This component is in the phase with permanent magnet flux. The second component, i_q current *produces an electromagnetic force.*

For rotor flux-oriented vector control of the LPMSM, the direct-axis stator current and the quadrature-axis stator current must be controlled independently. The electromagnetic force created by the motor is in *d_q* coordinate frame described by (4). This equation consists of two parts of the motor force. The first one '*magnetic*' is independent of the primary part current i_d, and is direct proportional to i_q current. The second part '*reluctance*' is proportional to both currents i_d, and i_q of the primary part multiplied by the difference between primary part self inductances in *d_q* axes (L_d - L_q). If the direct and quadrature inductances are the same or if the current component, i_d is kept at zero value by control law, the equation (4) then can be simplified, from which the most efficient control by controlling i_q current only, can be derived as it is describes in (5)

$$F=\frac{3}{2}\cdot K_x\cdot\left[\Psi_{PM}\cdot i_q+\left(L_d-L_q\right)\cdot i_d\cdot i_q\right] \tag{4}$$

$$F=\frac{3}{2}\cdot K_x\cdot\Psi_{PM}\cdot\left|I_s\right|\cdot\sin\alpha_m \tag{5}$$

where: α_m is the angle between vectors of primary part current $\mathbf{I_s}$ and permanent magnet flux $\mathbf{\Psi_{PM}}$ and $K_x=\pi/\tau_p$.

During such conditions that magnetic flux of permanent magnet, Ψ_{PM} is maintained constant, maximal force is achieved at angle $\alpha_m=90°$. This condition is satisfied for *d_q* coordinate system, which has d-axis identical with the direction of the permanent magnet flux and a primary part current vector $\mathbf{I_s}$ in this frame is orthogonal to d-axis and therefore i_d current will be 0. Controlling i_d current at zero value, the motor will produce maximal electromagnetic force up to the nominal velocity. If higher velocity than nominal is required then the field weakening must be applied by controlling the i_d

current as negative to keep approximately constant machine power.

Development of LPMSM Speed FDC Algorithm

Principles of feedback linearistion enable to formulate the linearising function for speed of the moving part, which forces this translational speed to obey specified closed-loop differential equation [3]. This equation, (6) is assumed linear, first order with a prescribed *time constant*, T_v . The computation technique for feedback linearisation is to equate the right hand side of (6) with the right hand side of the corresponding motor equation (2). This *forces* the non-linear differential equation (2) to have the same response as the linear equation (6). Thus:

$$a_{mp} = \frac{dv_{mp}}{dt} = \frac{1}{T_v}\left(v_d - v_{mp}\right) \tag{6}$$

$$\frac{1}{M}\left[c\left(\Psi_d i_q - \Psi_q i_d\right) - F_{ext}\right] = \frac{1}{T_v}\left(v_d - v_{mp}\right) \tag{7}$$

The second part of the control law is formulated on the principle of vector control, which requires mutual orthogonality between the rotor magnetic flux and stator current vectors. Following conventional approach, to achieve maximum magnetic flux up to nominal speed, the current demand, i_{d_d} for the magnetic flux component in direct axis is set to zero. Setting $i_d=0$ in (7) on the assumption that real current follows its demand, $i_d=i_{d\_d}$ and solving this equation for force producing component, i_{q_d} yields the following master control algorithm formulated for both stator current demands in the d_q-axis can be written:

$$i_{d\_d} = 0 \tag{8}$$

$$i_{q\_d} = \frac{1}{c\Psi_{PM}}\left[\frac{M}{T_v}\left(v_d - v_{mp}\right) + \hat{F}_{ext}\right] = \frac{Ma_{mp} + \hat{F}_{ext}}{c\Psi_{PM}} \tag{9}$$

Operational Control Modes

The numerator of the derived control algorithm (9) consists of two parts. The first one contains the demanded output acceleration and creates dynamic force during transients. The second part covers the external force, which needs to be estimated. By changing the prescribed acceleration, a_{mp} , various operational modes of the drive can be realised. Following modes were chosen as an example*:*

a) Direct acceleration control with constant acceleration, (10), *ramp*,
b) Direct acceleration control with linearly dependent acceleration, (11), *S-curve*,
c) Linear first order speed response, (12), *exponential*,
d) Second order speed response. (13), *fluent change of acceleration.*

$$a_d = \frac{v_d}{T_s}\operatorname{sgn}\left(v_d - v_{mp}\right) \tag{10}$$

$$a_d = \varepsilon t \cdot \operatorname{sign}\left(\omega_d - \omega_r\right) \quad \text{for } t \in \left(0, \frac{T_s}{2}\right) \tag{11}$$

$$a_d = \frac{1}{T_v}\left(v_d - v_{mp}\right) = \frac{3}{T_s}\left(v_d - v_{mp}\right) \tag{12}$$

$$\varepsilon = \frac{da_d}{dt} = \ddot{v}_{mp} = -2\xi\omega_n \dot{v}_{mp} + \omega_n^2\left(v_d - v_{mp}\right) \tag{13}$$

Ideal acceleration and speed responses based on described operational control modes are shown as the results of the overall FDC system simulations in Fig. 7. For the further work the second order speed response is encouraging due to benefit of fluent acceleration change and precisely defined speed and acceleration. New PIV controllers for position control of the drive, which is the next step of research, assume these variables as the inputs. Analysed versions of PIV position controller are shown in Fig. 3. The first version [4] operates with feedback from position and speed and the second version of such controller shown in Fig. 3b contains profile generator for generation of speed and acceleration feed-forward signals required for this controller.

FDC of LPMSM speed allows to replace whole speed control loop of the drive with first order delay, as it is described by (6), therefore simple proportional feedback can be exploited as position controller. This approach was already experimentally verified for near-time optimal position control of rotational drive with PMSM [5].

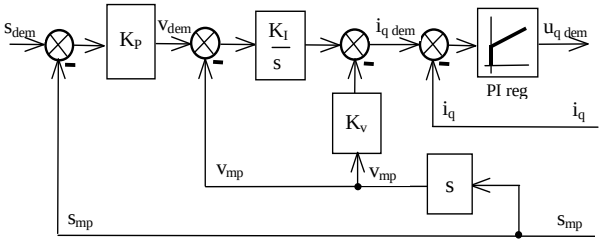

a) PIV position regulator

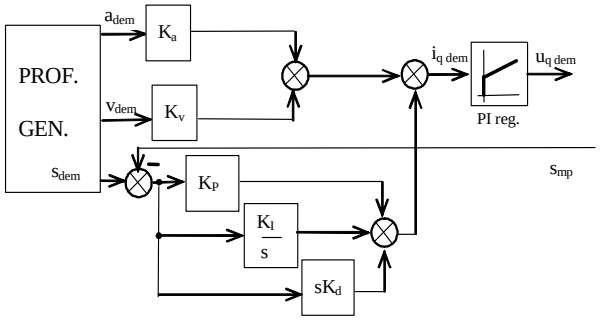

b) PIV position regulator with profile generator

Fig. 3 Position controllers for LPMSM Vector Control

Full-State Observer

The required speed, acceleration and external force as the inputs of the FDC master control algorithm are produced in observer. The observer, which exploits measurement of motor position, is full-state observer and provides all the estimates of aforementioned variables. Due to its filtering effect these variables can be exploited also for SVC position control of LPMSM. Thank to fact that external force is correctly estimated approximately in ten computational steps of control algorithm (*1 ms*) it can be exploited for diagnostic purpose too.

Real time model of observer is based on the motor position (1) and velocity (2) equations augmented by the third state equation for piecewise constant external force (17). The error (14) between real position and estimated position is added with corresponding gain into every correction loop of observer:

$$e_s = s_{mp} - \hat{s}_{mp} \tag{14}$$

$$\frac{d\hat{s}_{mp}}{dt} = \hat{v}_{mp} + K_s e_s \tag{15}$$

$$\frac{d\hat{v}_{mp}}{dt} = \frac{1}{M}\left[c\left(\Psi_d i_q - \Psi_q i_d\right) - \hat{F}_{ext}\right] + K_v e_s \tag{16}$$

$$\frac{d\hat{F}_{ext}}{dt} = 0 + K_F e_s \tag{17}$$

Block diagram of observer for estimates of external force, translational acceleration and speed of the moving part is shown in Fig. 4.

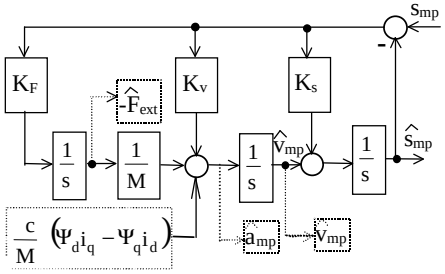

Fig. 4. Moving part speed and external force observer

The observer transfer function characteristic polynomial is given as LHS of (18) and if the observer poles are chosen as coincident and placed at $s=-6/T_{so}$ with settling time, T_{so}, which is RHS of (18), then by comparing both sides of (18) the observers gains are:

$$s^3 + s^2 K_s + sK_v + K_F / M = \\ = s^3 + \frac{18}{T_{so}} s^2 + \frac{108}{T_{so}^2} s + \frac{216}{T_{so}^3} \tag{18}$$

$$K_s = \frac{18}{T_{so}},\ K_v = \frac{108}{T_{so}^2} \text{ and } K_F = \frac{216M}{T_{so}^3} \tag{19}$$

The estimate, $\hat{F}_{ext}$ will follow arbitrary time varying external force and will do it more closely as T_{so} is reduced.

DESIGNED SYSTEM VERIFICATION

Verifications of the overall speed control system were performed in two steps. The first one was the verification by simulation of both control techniques (*SVC and FDC*) and the second step were the preliminary experiments with SVC of LPMSM.

The simulations of the design control system were performed with the LPMSM having parameters: P_n=800 W, p=3, r=0.156 m, R_s=0,59 Ω, L_d=3,7 mH, L_q=3.5 mH and Ψ_{PM}=0,3 Vs. The total load mass and external force are M=5 kg and F_{ext}=200 N. A sampling frequency of 10 kHz achieved during experiments with rotational PMSM was assumed also for the power electronics switches of inverter in simulation.

Simulations of SVC are arranged as preliminary experiments shown further and present the designed system response to a step speed demand of v_{dem}=1 ms^{-1} applied for time interval $t \in (0, 4]$ s, with zero initial states of all state variables followed immediately by opposite step speed demand of v_{dem}=-1 ms^{-1} applied for time interval $t \in [4\ \ 8)$ s. The external force F_{ext}=200 N is applied at t=2 s, which drops to zero at t=4 and at t=6 s is applied again. There is a change of sign for external force at t=6 s when speed is also negative. Simulation results for SVC show demanded speed, v_{dem}, and real speed of moving part, v_{mp} as subplot 5a and both current component together with applied F_{ext} as a functions of time as subplot 5b.

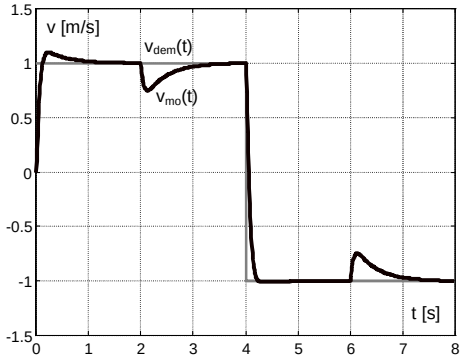

a) demanded and moving part speed

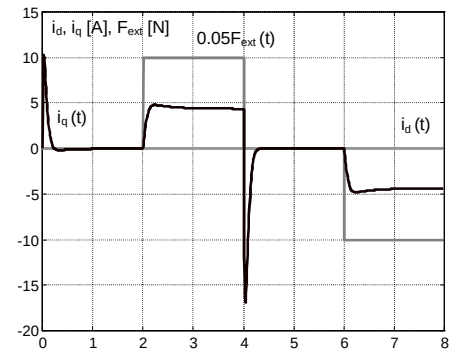

b) current components and applied external force

Fig. 5 Simulation of Vector Control of LPMSM

Preliminary experimental verifications are shown in Fig. 6 for similar conditions as for simulations. The measured response to a step speed demand of v_{dem}=1 ms^{-1} applied for time interval t∈(0, 4] s, followed immediately by opposite step speed demand of v_{dem}=-1 ms^{-1} applied for time interval t∈[4 8) s repeatedly.

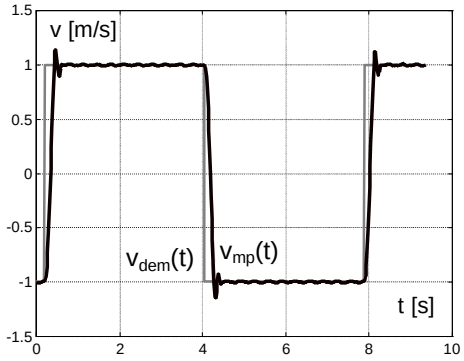

a) measured demanded and real speed

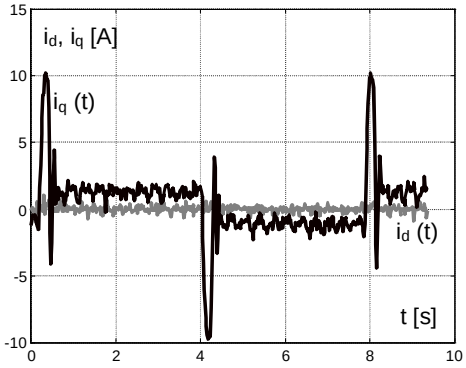

b) measured d_q current components

Fig. 6 Measured results for LPMSM SVC

As can be seen from Fig. 6 for speed measurement there are some overshoots in speed response due to mismatch of plant parameters. Measured current components confirm assumed functions and the proper operation of PI regulators.

Simulation of FDC for speed control of LPMSM with first order dynamics, ramp speed demand and second order dynamics are shown in Fig. 7. The left subplots show demanded speed, v_{dem} , and real speed of moving part, v_{mp} and right subplots show corresponding both current components with applied F_{ext} as a functions of time. Due to space limitation the simulation interval is 1 s only.

All the simulations show the FDC response to a step speed demand of v_{dem}=1 ms^{-1} applied for interval t∈(0, 0,5] s, with zero initial states of all state variables followed immediately by opposite step speed demand of v_{dem}=-1 ms^{-1} applied for time interval t∈[0,5 1) s. The external force F_{ext}=200 N is applied at t=0,3 s, which drops to zero at t=0,5 s and at t=0,8 s is applied again. There is a change of sign for external force at t=0,8 s when speed is also negative. As can be seen from individual subplots the ratio among the peak currents of the first order dynamic, subplot 7a, ramp speed demand, subplot 7b and the second order dynamic, subplot 7c is 3 : 1 : 1,5.

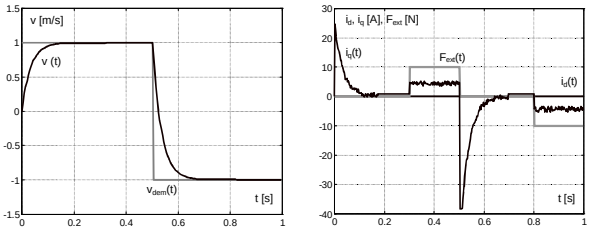

a) the first order dynamics

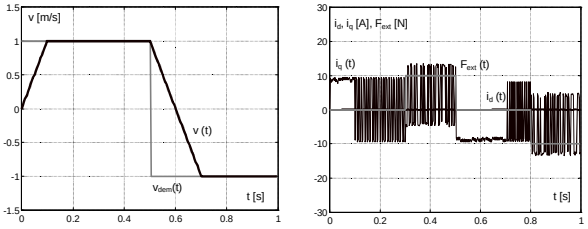

b) the ramp speed demand

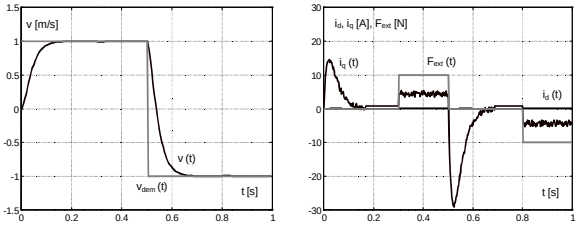

c) the second order dynamics

Fig. 7 Simulation of LPMSM Forced Dynamics Control

Based on theoretical predictions and simulations it was found that operational mode with second order dynamics enables fluent change of the load acceleration at relatively low current peak demand and therefore is very suitable for gentle handling of the load during speed transients.

EXPERIMENTAL BENCH WITH LPMSM

Linear PMSM shown in Fig. 8 was bought thanks to faculty funding from Baumueller Kamenz co. in 2006. This motor is composed of four pieces of primary part (B) and eight pieces of NeFeB permanent magnets (A). Total length of active path is 2640 mm and total length of mover is 660 mm. Primary parts are mounted on heavy duty aluminium profiles (D) to achieve firm base and good mechanical stability of the drive. Magnets are mounted on similar aluminium profiles (C). Linear movement is ensured with linear caged ball LM guide THK SSR 35 (E-F). For position measurement the linear magnetic position sensor LS100 + MB100, (G) from SIKO GmbH with 10 μm accuracy is mounted on the base of the motor. Output signal of position sensor is analogical to resolver (*with sine and cosine functions*) and period of signals is 1 mm. Very important accessories in the system are mechanical (I) and electrical (H) safety parts.

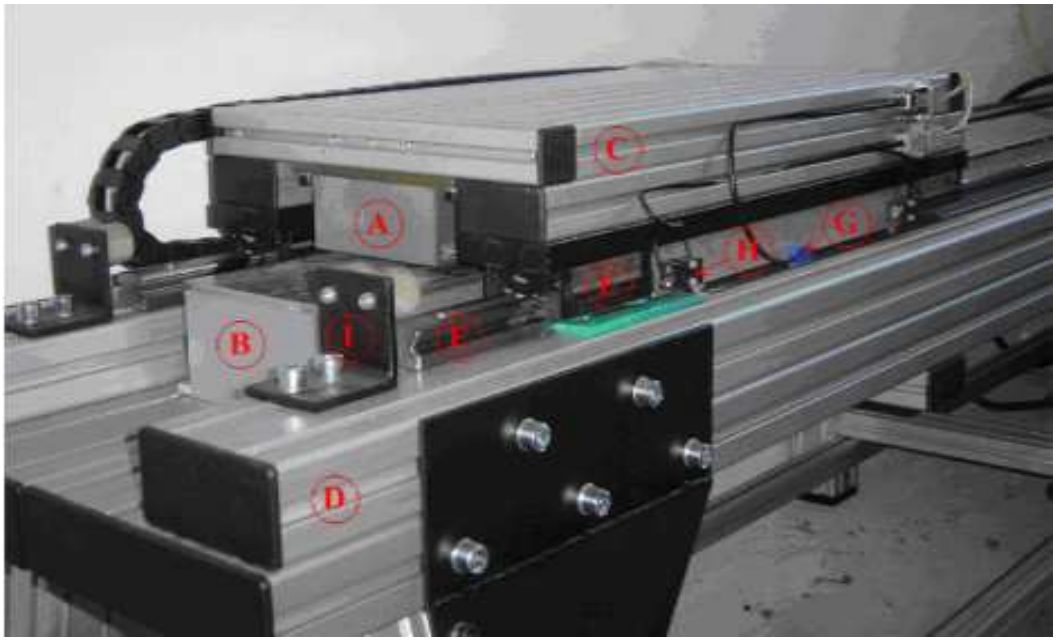

Fig. 8 Experimenal bench with LPMSM

CONCLUSIONS AND SUGGESTIONS FOR FURTHER WORK

The presented simulation and preliminary experimental results indicate that both designed speed control systems for the electric drives exploiting LPMSM operate properly.

It can be observed from Fig. 7, subplot a) for the first order dynamics, subplot b) ramp speed demand and subplot c) second order speed demands that prescribed dynamics were achieved including prescribed settling time as it was intended.

The preliminary experimental results with SVC of LPMSM shown in Fig. 6 indicate that the designed PI controllers operate properly with realistic errors in the assumed motor parameters. Results are presented as preliminary due to operation without external load force. More suitable adjustment of PI regulator can bring further improvement of the control circuitry.

The experimental verification of the designed FDC system, including operation of observer should be sought as a continuation of this work.

ACKNOWLEDGMENT

The authors wish to thank Slovak Grant Agency VEGA for funding the project No. 4087/07 'Servosystems with rotational and linear motors without position sensor'.

REFERENCES

[1] I. Boldea, S.A. Nasar, *Vector Control of AC Drives*, 2nd edition, CRC Press, 1992

[2] A. Isidori, *Nonlinear Control Systems*, Springer-Verlag, Berlin, DE: 1989.

[3] J. Vittek, S.J. Dodds. *Forced Dynamics Control of Electric Drives*, EDIS Zilina, SK, 2003, http://www.kves.uniza.sk/

[4] M. Žalman, J. Jovankovič, *New trends in control of linear motors*, AT&P Journal 2/2006, pp. 67–70.

[5] J. Vittek, T. Baculak, S.J. Dodds, R. Perryman. Near-Time-Optimal Position Control of Electrical Drives with Permanent Magnet Synchronous Motor, *Proceedings of the EPE Conference*, Toulouse, France, 2003.

[6] N.S. Nise. *Control System Engineering*, The Benjamin Cumming Co., Redwood, CA, 1995.

[7] S.J. Dodds, H. Wild, Real-time Identification of the Friction Coefficient of a Rolling Guided High Dynamic Linear Motor," *Proc. of the* Control'98 *Conference*, United Kingdom, 1998.

[8] K. Urbanski, K. Zawirski, Sensorless Control of SMPM with Modified Observer Structure, in *Proceedings of the EPE-PEMC Conference*, Cavtat, Croatia, 2002.

[9] D. Perdukova, P. Fedor, J. Timko, "Modern Methods of Complex Drives Control," *Acta Technica CSAV* vol. 49, Czech Republic, 2004, pp. 31-45.

[10] G. Knerczer, L. Nagy, P. Korondy, S. Peresztegi, T. Mezo: "Compact Motors and Drives for Electric Vehicles", *Automatika*, vol.45, No.1-2, 3004, Croatia, pp.47-55.